Effective Dielectric Properties of Biological Cells: Generalization of the Spectral Density Function Approach

ARTICLE *in* THE JOURNAL OF PHYSICAL CHEMISTRY B · AUGUST 2009

Impact Factor: 3.3 · DOI: 10.1021/jp900703a · Source: PubMed

2 AUTHORS:

Anatoliy Goncharenko
National Cheng Kung University
68 PUBLICATIONS **458** CITATIONS
SEE PROFILE

Yia Chang
Academia Sinica
390 PUBLICATIONS **5,139** CITATIONS
SEE PROFILE

Effective Dielectric Properties of Biological Cells: Generalization of the Spectral Density Function Approach

Anatoliy V. Goncharenko*,†,‡,§ and Yia-Chung Chang†

Research Center for Applied Sciences, Academia Sinica, Nankang, Taipei 115, Taiwan, ROC; Department of Physics, National Cheng-Kung University, Tainan, Taiwan, ROC; and Institute of Semiconductor Physics, National Academy of Sciences of Ukraine, 03028, Kyiv, Ukraine

Received: January 23, 2009; Revised Manuscript Received: May 20, 2009

We suggest an extension of the spectral density function approach to describe the complex dielectric response of suspensions of arbitrarily shaped particles having a thin shell, in particular, biological cells. The approach is shown to give analytical results in some simple but practically important cases. In the general case, for the 3-phase systems it reduces to determination of the spectral density function for the suspension of a certain kind. Prospects and limitations of the approach, as well as practical examples, are also considered.

I. Introduction

Today's dielectric spectroscopy is a powerful tool to study mechanisms of the interaction of electromagnetic fields with biocells, enabling one to consider the influence of various physical and chemical factors on the cell dielectric properties. Actually, dielectric impedance measurements are simple, fast, and not invasive. As a result, the use of the spectroscopy in biological studies and biotechnology industries is increasing.[1] At the same time, in some cases its practical implementation involves difficulties that, in turn, requires a further elaboration of underlying models. Indeed, on the one hand, there are a number of well-developed numerical techniques, such as the finite element method, finite-difference time-domain method, multiple multipole method, rigorous coupled wave analysis, etc. However, numerical techniques are frequently time-consuming, especially due to very different length scales for the cell size and the membrane thickness. For example, although the typical size of the red blood cells is on the order of 10 μm, the membrane thickness is on the order of only 10 nm. In addition, numerical techniques are sometimes unstable and inconvenient when the need arises to investigate behavior of the dielectric response depending on model parameters. On the other hand, there are some simple classical models allowing one to obtain analytical results for the dielectric response. The widely used classical model involves consideration of two confocal ellipsoidal layers, the cytoplasm and the membrane; an extension to multishell ellipsoid model is also possible.[2] Although such a model considerably simplifies calculations, its practical use is frequently limited due to unrealistic, oversimplified geometry. Real biocells come in a variety of shapes. So, bacteria can take much more complicated shape, such as, for example, rod-like, curved or spiral, croissant, wavy, etc.[3] In these cases the ellipsoidal shape assumption is poor. However, so far only a few (mainly numerical) studies were beyond the scope of the ellipsoidal model. Among them, mention may be made of two methods feasible for dilute suspensions of axially symmetric biocells;[4,5] a review on numerical methods as applied to dielectric mixtures is given by Tuncer et al.[6] So the further progress of the dielectric spectroscopy has motivated a growing need for accurate and efficient modeling allowing one to correctly describe the dielectric properties of the cells.

In this paper, we develop the spectral density function approach, pioneered by Bergman[7] and Milton,[8] for studying the biological cell suspensions. At present, the approach is widely used to describe the effective dielectric and optical properties of various inhomogeneous media, including cell suspensions.[9] Its main advantage is that it allows one to separate the material parameters (permittivities and/or conductivities) and the microgeometrical parameters of the media. At the same time, there is a serious restriction of the method, lying in the fact that its use involves difficulties when dealing with media consisting of more than two phases. Two known exceptions are dilute suspensions of the shelled spheroids[10] and of the graded (or multilayered) spheres.[11] In other words, the spectral representation in its conventional form is applicable for two-phase composite systems only. The primary purpose of this paper is to extend the spectral representation for the effective dielectric constant of two-phase media to more complicated multiphase systems such as biological cell suspensions.

II. Basic Formalism

Before consideration of three-phase composites, let us first consider the case of the two-phase ones. Actually, there are two forms of the spectral density formalism. Besides, there is Fuchs' representation, which looks very similar to the above formalism.[12] Sometimes this fact leads to some misunderstanding. To avoid confusion, we briefly discuss these issues here.

Ronald Fuchs showed that the complex dielectric susceptibility of a small arbitrarily shaped particle can be written as a sum over its normal modes. Making use of this fact, he also obtained an expression for the effective dielectric constant of a dilute suspension of the well-separated particles.[12] It should be noted that Fuchs' result was derived without taking into account interparticle interactions.

The spectral representation for the effective dielectric constant was originally formulated in the form of the sum:[7]

* To whom correspondence should be addressed. E-mail: anatolii@mail.ncku.edu.tw.
† Academia Sinica.
‡ National Cheng-Kung University.
§ National Academy of Sciences of Ukraine.

10.1021/jp900703a CCC: $40.75
Published on Web 07/01/2009

$$\varepsilon_{\text{eff}} = \varepsilon_0\left(1 + f_1 \sum_n \frac{F_n}{s_n - s}\right) \quad (1)$$

where f_1 is the volume fraction of the phase 1, $s = \varepsilon_0/(\varepsilon_1 - \varepsilon_0)$, and ε_0 and ε_1 are the complex relative dielectric constants of the phases (for the sake of definiteness, in the following the phase 0 is considered to be a host or, in biological terms, an extracellular medium). Conventionally, eq 1 is supplemented with the sum rules $\sum_n F_n = 1$ and $\sum_n F_n s_n = (1 - f_1)/3 = f_0/3$. All the complex dielectric constants ε_0, ε_1, and ε_{eff} may be defined in terms of the corresponding relative permittivities ε'_k and conductivities σ_k as $\varepsilon_k = \varepsilon'_k - i\varepsilon''_k = \varepsilon'_k - i\sigma_k/\varepsilon_v\omega$, where $k = 0, 1, 2$, eff and ε_v is the free space permittivity.

Later, Golden, and Papanicolaou[13] noticed that the distribution of the poles in eq 1 can be continuous. If so, the integral form of the spectral representation

$$\varepsilon_{\text{eff}} = \varepsilon_0[1 + f_1 \int_0^1 g(x)p(x)\,dx] \quad (2)$$

with $g(x)$ the spectral density function and $p(x) = (s + x)^{-1}$, seems to be more convenient. Equation 2 is supplemented with $\int_0^1 g(x)\,dx = 1$ and $\int_0^1 xg(x)\,dx = f_0/3$. It should be, however, noted that both forms of the spectral representation, eqs 1 and 2, are equivalent if to assume that

$$g(x) = \sum_n F_n \delta(x - s_n) \quad (3)$$

where $\delta(...)$ is the Dirac delta function.

Let us now take a closer look at eq 2. It is easily seen that $p(x)$ may be considered as a dimensionless polarizability of a single spheroid having the dielectric constant ε_1 and the depolarization factor x along its axis of revolution. More exactly, $p(x)$ is one of diagonal components of the dimensionless polarizability tensor corresponding to orientation of the incident electric field along the spheroid symmetry axis. It means that formally the effective linear response of an arbitrary two-phase isotropic composite is the same as one of the diagonal components of the effective linear response tensor of a system of equally oriented and noninteracting spheroids possessing a shape distribution.[14] Thus, instead of consideration of a suspension of arbitrarily shaped particles with a complicated geometry, determination of the effective dielectric constant may be reduced to consideration of a relatively simple suspension of shape-distributed spheroids.

Consider now a composite consisting of shelled (core−shell) spheroids. A natural idea suggesting itself now is to extend eq 2, substituting $p(x)$ with the dimensionless polarizability $p^*(x)$ of the shelled spheroid and f_1 with the volume fraction of the shelled spheroid $f = f_1 + f_2$:

$$\varepsilon_{\text{eff}} = \varepsilon_0[1 + f \int_0^1 g(x)p^*(x)\,dx] \quad (4)$$

where f_1 and f_2 are the volume fractions of a shell and a core, respectively; the volume fraction of a host is $f_0 = 1 - f = 1 - f_2 - f_1$. To do this, we could introduce an equivalent dielectric constant ε_e of the shelled spheroid and then

$$p^*(x) = \{[\varepsilon_e(x)/\varepsilon_0 - 1]^{-1} + x\}^{-1} \quad (5)$$

The value of ε_e is such that if the dielectric constant of the surrounding ε_0 is equal to it, then the field and the potential at any point in the medium is unperturbed by the introduction of the shelled spheroid. Both the size and shape of the equivalent spheroid are considered to be the same as those of the original shelled spheroid. It should be noted that when using such a definition, the internal electric field of the equivalent spheroid may be treated as constant independently of the spheroid concentration. This is so because the above formalism considers the spheroids to be noninteracting.

It is clear that doing so allows us to extend the spectral representation to a class of the three-phase composites. A question, of course, appears what the class is. Rigorous and comprehensive consideration of this problem does not seem to be straightforward and is beyond the scope of the present paper (we are going to consider it in more detail elsewhere). It is reasonable to assume, however, that this class includes the core−shell particle composites as a subset. The arguments to support this claim can be as follows. Earlier, it was shown that there is an equivalence between a shelled (inhomogeneous) particle and a homogeneous one having the same size and shape.[15] In other terms, there exists a charge distribution on the external surface of the shell that results in the true electrical field outside the particle. It means that we may introduce an equivalent permittivity of the shelled particle considering it to be homogeneous. It should be also noted that the validity of the above assumption regarding consideration of the permittivity of coated particles in terms of the effective medium theory was supported experimentally for a dilute suspension of slightly deformed coated spheres.[16] Thus, dealing with a suspension we may replace the real core−shell particles by the homogeneous ones. As to the suspension of the homogeneous particles, we can now use the spectral density representation.

To proceed further, we need to know the polarizability p^* of the shelled spheroid. Analytically, the problem can be solved using the separation of variables method in spheroidal coordinates.[17] It is possible, however, only if both spheroids (inner and outer) are to be confocal. The resulting expression for diagonal components of the polarizability tensor involves the corresponding depolarization factors of the core (L_2) and the shell (L_1). In many papers it is mistakenly assumed that $L_2 = L_1$. This assumption, in general, is not correct for the confocal spheroids.[18,19] Indeed, if L_1 and q are specified, the depolarization factor L_2 of the outer spheroid should depend on the volume ratio of the core to the whole spheroid $q = f_2/(f_1 + f_2)$. So, $L_1 \approx L_2$ only for sphere-like particles, when $L_1 \approx L_2 \approx 1/3$, or if $q \to 1$, that is, in the limit of very thin shells. In fact, the latter is indeed the case when dealing with biocells. Due to this, we consider this issue in more detail.

Let a shelled spheroid have the above-mentioned depolarization factors L_1 and L_2 along its axis of revolution. Then, the equivalent dielectric constant of the spheroid may be written as (see, e.g., ref 20, where we have revised an obvious misprint in the numerator)

$$\varepsilon_e = \varepsilon_1 \frac{qL_1 - L_2 - q - s_{12}}{qL_1 - L_2 - s_{12}} = \varepsilon_1\left(1 - \frac{q}{qL_1 - L_2 - s_{12}}\right) \quad (6)$$

with $s_{12} = \varepsilon_1/(\varepsilon_2 - \varepsilon_1)$, ε_1, and ε_2 the dielectric constants of the shell and the core, respectively. Furthermore, it is clear that the above formalism may be easily extended to the case of multishelled spheroids using an obvious iterative procedure.

Then, equating the depolarization factors of all spheroids, that is, taking $L \equiv x = L_1 = L_2 = ... = L_{N-1}$, one has a set of N iterative equations for the determination of the equivalent permittivity of the N-shelled spheroid

$$\varepsilon_e = \varepsilon_1\left[1 + \frac{q_2}{L(1 - q_2) + \varepsilon_1/(\varepsilon_{2e} - \varepsilon_1)}\right] \quad (7a)$$

$$\varepsilon_{2e} = \varepsilon_2\left[1 + \frac{q_3}{L(1 - q_3) + \varepsilon_2/(\varepsilon_{3e} - \varepsilon_2)}\right] \quad (7b)$$

and so on, up to

$$\varepsilon_{Ne} = \varepsilon_N\left[1 + \frac{q_{N+1}}{L(1 - q_{N+1}) + \varepsilon_N/(\varepsilon_{N+1} - \varepsilon_N)}\right] \quad (7c)$$

III. Particular Examples of the Spectral Density Function

For illustration purposes, let us consider some simple examples setting particular forms of the spectral density function.

i. $$g(x) = \delta(x - 1/3) \quad (8)$$

It is easily seen that such a choice results in the well-known expression for the effective dielectric constant of the shelled spheres in the dilute limit:[21]

$$\varepsilon_{eff}/\varepsilon_0 = 1 + 3(f_1 + f_2) \times \frac{(\varepsilon_1 - \varepsilon_0)(\varepsilon_2 + 2\varepsilon_1) + q(\varepsilon_2 - \varepsilon_1)(\varepsilon_0 + 2\varepsilon_1)}{(\varepsilon_1 + 2\varepsilon_0)(\varepsilon_2 + 2\varepsilon_1) + 2q(\varepsilon_2 - \varepsilon_1)(\varepsilon_1 - \varepsilon_0)} \quad (9)$$

ii. $$g(x) = \delta(x - f_0/3) \quad (10)$$

Such a choice yields an extension of the Maxwell-Garnett approximation to the shelled spheres

$$\varepsilon_{eff}/\varepsilon_0 = 1 + \frac{f_1 + f_2}{(\varepsilon^* - 1)^{-1} + f_0/3} \quad (11)$$

with

$$\varepsilon^* = \varepsilon_1\left(1 - \frac{3q}{qf_0 - f_0 - 3s_{12}}\right)$$

iii. In real practice, the shape of biological cells can vary from cell to cell. If so, it looks natural to consider an extended spectral density function. The simplest example describing the uniform distribution of ellipsoidal shapes around the spherical shape is the rectangular (step-like) function of the form[14]

$$g(x) = \begin{cases}\Delta^{-1}, \text{if } \frac{1}{3}f_0(1 - \Delta) < x < \frac{1}{3}f_0(1 - \Delta) + \Delta \\ 0, \text{otherwise}\end{cases} \quad (12)$$

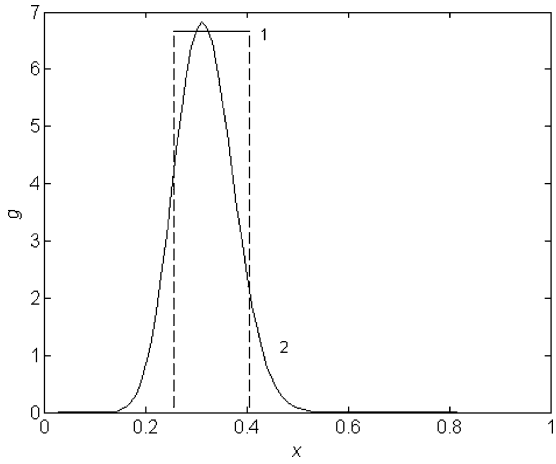

Figure 1. Examples of the spectral density function: eq 12 with $f_0 = 0.9$, $\Delta = 0.15$ (1) and eq 16 with $f = 0.05$, $\alpha = 20$ (2).

where Δ is the width of the function (see Figure 1); if now Δ approaches 0, eq 12 transforms into eq 10. As to the effective dielectric constant, it takes the analytical form

$$\varepsilon_{eff}/\varepsilon_0 = 1 + \frac{f_1 + f_2}{\Delta} \times \left\{\frac{1}{2}\ln\frac{[f_0(1 - \Delta) + 3\Delta]^2 + b[3f_0(1 - \Delta) + 9\Delta] + 9c}{f_0^2(1 - \Delta)^2 + 3f_0b(1 - \Delta) + 9c}\right\} - \frac{r}{t}\ln\left[\frac{2f_0(1 - \Delta) + 6\Delta + 3b - 3t}{2f_0(1 - \Delta) + 6\Delta + 3b + 3t}\cdot\frac{2f_0(1 - \Delta) + 3b + 3t}{2f_0(1 - \Delta) + 3b - 3t}\right] \quad (13)$$

where

$$b = s_{01} + \frac{qs_{10} - s_{12}}{1 - q}, c = \frac{s_{01}s_{12}}{1 - q}, t = \sqrt{b^2 - 4c},$$
$$r = \frac{b}{2} - \frac{qs_{10} + s_{12}}{1 - q}, s_{01} = \frac{\varepsilon_0}{\varepsilon_1 - \varepsilon_0}$$

and $s_{10} = (\varepsilon_1)/(\varepsilon_0 - \varepsilon_1)$. It is worth noting that the parameter Δ may be considered as a measure of cells' nonsphericity.

iv. To extend the Maxwell−Garnett approximation to a suspension of the randomly oriented shelled spheroids, it is convenient to adopt the known result for the bare spheroids:[22]

$$g(x) = F_1\delta(x - s_1) + F_2\delta(x - s_2) \quad (14)$$

where

$$s_1 = \frac{1}{4}\left[1 - \frac{2}{3}f + L + \frac{1}{3}\sqrt{(2f - 3 - 3L) - 72f_0(1 - L)L}\right]$$

$$s_2 = \frac{1}{4}\left[1 - \frac{2}{3}f + L - \frac{1}{3}\sqrt{(2f - 3 - 3L) - 72f_0(1 - L)L}\right],$$
$$F_1 = \frac{1 + 3L - 6s_1}{6(s_2 - s_1)}, F_2 = \frac{1 + 3L - 6s_2}{6(s_1 - s_2)}$$

and L is the depolarization factor of spheroids along the symmetry axis. In this case the effective dielectric constant takes the form

$$\varepsilon_{\text{eff}}/\varepsilon_0 = \frac{1 + f[(1 - L)\beta_{||} + (1 + L)\beta_{\perp}]/3}{1 - f[L\beta_{||} + (1 - L)\beta_{\perp}]/3} \quad (15)$$

where

$$\beta_{||} = \frac{\varepsilon_e^{||} - \varepsilon_0}{\varepsilon_0 + L(\varepsilon_e^{||} - \varepsilon_0)},\ \beta_{\perp} = \frac{\varepsilon_e^{\perp} - \varepsilon_0}{\varepsilon_0 + (1 - L)(\varepsilon_e^{\perp} - \varepsilon_0)/2},$$
$$\varepsilon_e^{||} = \varepsilon_1\left(1 - \frac{q}{qL - L - s_{12}}\right)$$

and

$$\varepsilon_e^{\perp} = \varepsilon_1\left[1 - \frac{q}{(q - 1)(1 - L)/2 - s_{12}}\right]$$

v. From the physical point of view, it is more justified to speak about the continuous and smooth spectral density function. The simplest example resulted from delta function broadening due to various physical mechanisms, including both mutual interaction and shape fluctuation of the particles, is the single-mode approximation in the form of the Beta distribution

$$g(x) = B^{-1}(\alpha, \beta)x^{\alpha-1}(1 - x)^{\beta-1} \quad (16)$$

where $B(...)$ is the Beta function and $\beta = \alpha(2 + f)/(1 - f)$ in the three-dimensional case[23,24] (see Figure 1). Upon substitution of eq 16 into eq 4, the effective dielectric constant may be easily obtained; in the two-phase case it is shown to agree with experimental spectra of brine-saturated rocks.[23] The approximation (eq 16) may be considered as a particular case of a more general approximation for the spectral density function in the form of a sum of the Beta distributions.[24]

vi. For some bioapplications, the Looyenga equation $\varepsilon_{\text{eff}} = (\sum_i f_i \varepsilon_i^{1/3})^3$ and Kraszewski equation $\varepsilon_{\text{eff}} = (\sum_i f_i \varepsilon_i^{1/2})^2$ are shown to be useful.[25,26] One can show that the spectral density function corresponding to these equations in our case may be written as

$$g(x) = \frac{1}{\pi f}[f_0^2 + f_0 f t^{1/3} + f^2 t^{2/3}]^{3/2}\sin(3\phi) \quad (17)$$

and

$$g(x) = \frac{2}{\pi} f_0 t^{1/2} \quad (18)$$

respectively, where $\phi = \arctan[(ft^{1/3})/(2f_0 + ft^{1/3})]$, $t = (1/x) - 1$. We note that both equations are particular cases of the more general Lichtenecker equation for which the spectral density function is also known.[27]

vii. One of the most popular is the Bruggeman−Hanai equation, which has proved to work very well for concentrated suspensions of spheres with a volume fraction up to 0.8.[2] In our case the equation may be written as $f_0 = (\varepsilon_{\text{eff}} - \varepsilon^*)/(\varepsilon_0 - \varepsilon^*)(\varepsilon_0/\varepsilon_{\text{eff}})^{1/3}$. The spectral density function corresponding to the Bruggeman−Hanai equation for two-phase systems is known.[28] In our case, the function takes the form

$$g(x) = \begin{cases} \frac{\sqrt{3}}{2\pi}\frac{f_0}{f}\left(\frac{1 - x}{2x^4}\right)^{1/3}[(1 + B)^{1/3} - (1 - B)^{1/3}],\ x_l < x < x_u \\ 0,\ \text{otherwise} \end{cases} \quad (19)$$

where

$$B = \sqrt{1 - \frac{4f_0^3}{27x(1 - x)^2}},\ x_l = \frac{2}{3}\left[1 - \cos\left(\frac{\pi - \varphi}{3}\right)\right],$$
$$x_u = \frac{2}{3}\left[1 - \cos\left(\frac{\pi + \varphi}{3}\right)\right]$$

and

$$\varphi = \arccos(2f_0^3 - 1)$$

IV. Practical Examples

To demonstrate the potential and versatility of our approach, consider some practical examples. The first example shows the effect of the shape distribution or, more exactly, fluctuation of the cell shape around the most probable spherical shape on the effective dielectric properties of a suspension of human leukocytes. This choice is motivated by the fact that normal human leukocytes are known to have near-spherical shape and, in addition, may be described in terms of the single-shell model.[29,30] To be more specific, consideration is given to a water suspension of T-lymphocytes. The model parameters have been taken as follows: the cell volume fraction $f = 0.15$, the cell membrane thickness $d = 4.5$ nm, $f_1 = 0.005$, $\varepsilon'_0 = 80$, $\sigma_0 = 0.056$ S/m, $\varepsilon_1 = (C_s/\varepsilon_v - jG_s/\varepsilon_v\omega)d$ with $C_s = 12$ mF/m^2 and $G_s = 100$ S/m^2, $\varepsilon'_2 = 74$, $\sigma_2 = 1$ S/m. The above cell parameters are typical for human T-lymphocytes.[30] First, we used eq 11 to compute the frequency dependencies of the effective permittivity $\varepsilon^0_{\text{eff}}(\omega) = \varepsilon'_{\text{eff}}(\omega, \Delta = 0)$ and conductivity $\sigma^0_{\text{eff}}(\omega) = \sigma_{\text{eff}}(\omega, \Delta = 0)$ in the spherical approximation. Then, we used eq 13 and found the same dependencies at different values of the nonsphericity parameter Δ. The results for the normalized dependencies $\varepsilon'_{\text{eff}}(\omega, \Delta)/\varepsilon^0_{\text{eff}}(\omega)$ and $\sigma_{\text{eff}}(\omega, \Delta)/\sigma^0_{\text{eff}}(\omega)$ are shown in Figure 2. We see that at the chosen parameters the effect of the nonsphericity on the effective dielectric response is weak but can be noticeable; so, at $\Delta = 0.1$ (this corresponds to a moderate nonsphericity) a deviation of both $\varepsilon'_{\text{eff}}(\omega,\Delta)$ and $\sigma_{\text{eff}}(\omega,\Delta)$ from their values in the spherical approximation can reach 3%. At the same time, both $\varepsilon'_{\text{eff}}(\omega, \Delta)/\varepsilon^0_{\text{eff}}(\omega)$ and $\sigma_{\text{eff}}(\omega,\Delta)/\sigma^0_{\text{eff}}(\omega)$ reveal completely different frequency dependencies. For example, at about 7×10^7 Hz the effect of nonsphericity on σ_{eff} is maximal, whereas the same effect on $\varepsilon'_{\text{eff}}$ is close to zero. For completeness, Figure 3 gives the normalized Cole−Cole diagrams, $\sigma_{\text{eff}}(\omega, \Delta)/\sigma^0_{\text{eff}}(\omega)$ vs $\varepsilon'_{\text{eff}}(\omega, \Delta)/\varepsilon^0_{\text{eff}}(\omega)$, at different values of the parameter Δ. It shows how the diagrams shrink to the point (1, 1) when $\Delta \to 0$.

In the next example we consider the electrical properties of human erythrocytes (red blood cells). The typical dielectric spectra of an erythrocyte suspension with $f = 0.15$ measured at $T = 37$ °C and corrected for the electrode polarization effect are given in Figure 4. The electrical parameters of the extracellular medium (ε_0 and σ_0) were measured directly. The theoretical dependence $\varepsilon_{\text{eff}}(\omega)$ was computed with the use of eqs 4 and 16. To do it, we had fixed the parameter $q = 0.9967$[31]

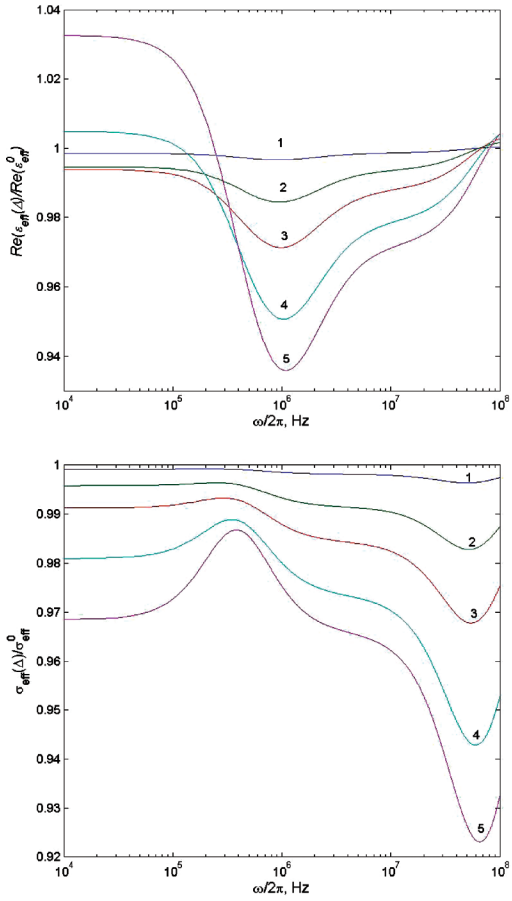

Figure 2. Frequency dependences of the effective permittivity and conductivity for shape-distributed cell suspensions normalized to the corresponding permittivity and conductivity for spherical cells at several values of the nonsphericity parameter: $\Delta = 0.01$ (1), 0.05 (2), 0.1 (3), 0.2 (4), and 0.3 (5).

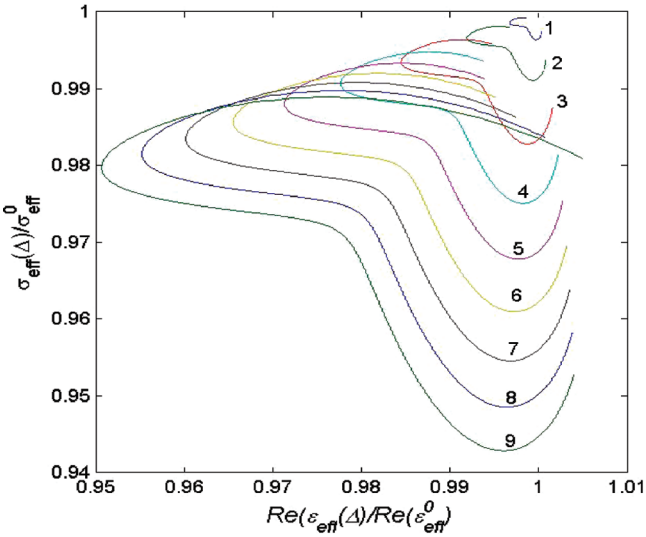

Figure 3. The normalized Cole−Cole diagrams $\sigma_{eff}(\Delta)/\sigma^0_{eff}$ vs $\varepsilon'_{eff}(\Delta)/\varepsilon^0_{eff}$ for the same suspension at $\Delta = 0.01$ (1), 0.025 (2), 0.05 (3), 0.075 (4), 0.1 (5), 0.125 (6), 0.15 (7), 0.175 (8), and 0.2 (9).

and the cytosol permittivity ($\varepsilon_2 = 150$).[25] Four other parameters (α, ε_1, σ_1, and σ_2) were fitted to experimental data. As seen from Figure 4, the best-fit curves, obtained by minimizing the residual function $R = \sum[\mathrm{Re}(\varepsilon^{exp}_{eff} - \varepsilon^{fit}_{eff})]^2/\sum(\varepsilon^{exp}_{eff})^2 + \sum(\sigma^{exp}_{eff} - \sigma^{fit}_{eff})^2/\sum(\sigma^{exp}_{eff})^2$ with $\sigma_{eff} = \varepsilon_\nu \omega \mathrm{Im}(\varepsilon_{eff})$, show a reasonable agreement between the experimental and calculated results. It

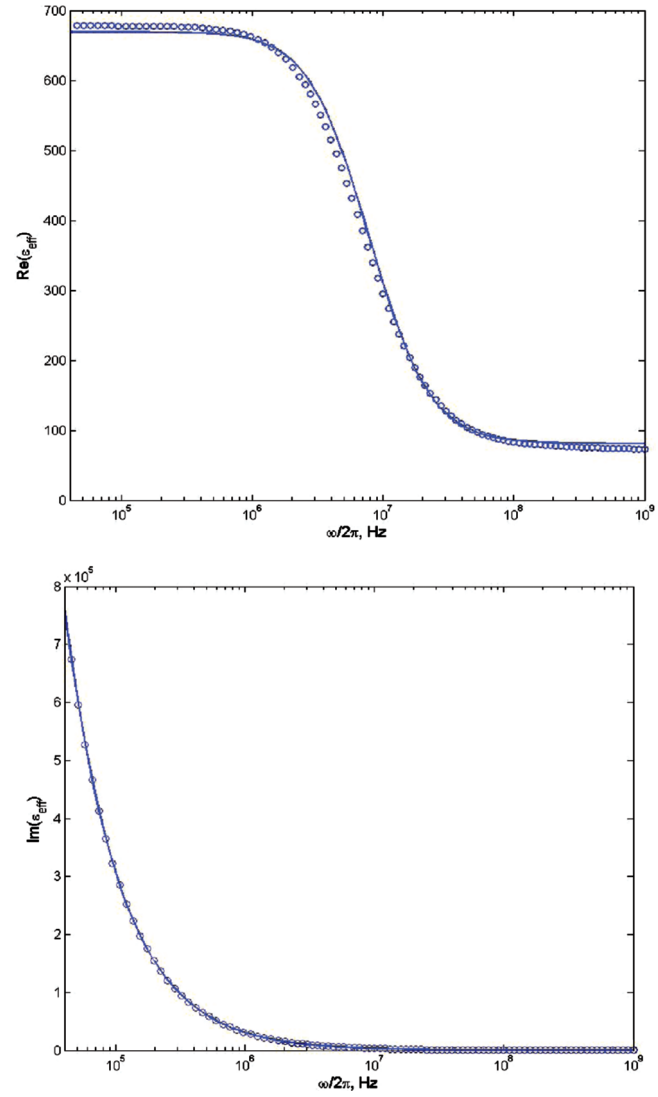

Figure 4. The dielectric spectra of a suspension of human erythrocytes. The solid lines are the best-fit curves obtained at $\alpha = 0.231$, $\varepsilon_1 = 4.88$, $\sigma_1 = 76 \times 10^{-5}$ S/m, and $\sigma_2 = 2.28$ S/m with the corresponding value of the residual function $R = 9.3 \times 10^{-4}$.

should be noted that our value of the membrane permittivity ($\varepsilon_1 = 4.88$) is in good agreement with that obtained in ref 31. Besides, a 5-fold decrease in the cytosol permittivity (which, generally speaking, is known with a large uncertainty) results in only a slight change of the fitted parameters. So, in this case we have obtained $\alpha = 0.28$, $\varepsilon_1 = 4.58$, and $\sigma_2 = 2.37$ S/m. As to the value of the membrane conductivity, it remains almost unchanged. Within the framework of our model, the relative errors can be estimated as 15% for α, 6% for ε_1, and 4% for σ_2.

Our last example involves a more complicated geometry, namely, doublet (budding) cells. A typical instance of this kind of geometry is budding yeast in cell separation.[32] Because the quantitative analysis of the dielectric properties of yeast cell suspensions is troublesome due to many unknown parameters, here we consider the problem qualitatively.

In the previous experimental study, it was shown that for the cells accumulated as doublets immediately before cell separation, one more subdispersion occurs in addition to two dielectric dispersions taking place for the single cells without bud.[32] This feature was attributed to the specific shape of the doublet cells when both the parent and bud cells are in

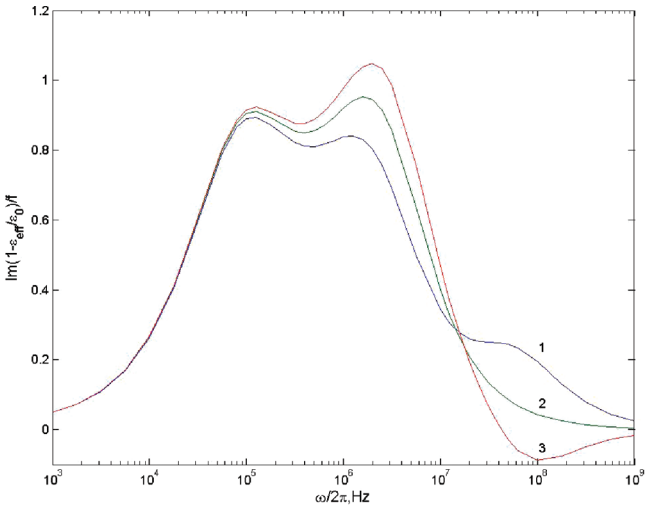

Figure 5. The behavior of the function $T = f^{-1}\mathrm{Im}\ (1 - \varepsilon_{\mathrm{eff}}/\varepsilon_0)$ at different values of the cytosol conductivity: $\sigma_2 = 0.2$ S/m (1); $\sigma_2 = 0.3$ S/m (2); $\sigma_2 = 0.2$ S/m (3).

electrical contact.[33] To model the corresponding geometry, we use the two-mode spectral density function of the form $g(x) = \sum_{i=1}^{2} C_i x^{\alpha_i - 1}(1-x)^{\beta_i - 1}$ which involves four free parameters.[24] For illustration purposes and for comparison with the above paper by Sekine et al.,[33] who made use of the boundary element method, our results are presented in terms of the function $T = f^{-1}\mathrm{Im}\ (1 - \varepsilon_{\mathrm{eff}}/\varepsilon_0)$. To obtain a good agreement, we have fixed the material parameters as in ref 32 ($\varepsilon_0 = \varepsilon_2 = 80$, $\varepsilon_2 = 5.5$, $\sigma_0 = 0.3$ S/m, $\sigma_1 = 0$) and the geometry parameters as $\alpha_1 = 0.7$, $\beta_1 = 1.44$, $\alpha_2 = 890$, $\beta_2 = 7$. In accordance with ref 33, the parameter q is chosen as 0.986 and the cell volume fraction $f = 0.001 \ll 1$ (under this condition, the spectral density function is almost independent of f). After that, we consider the effect of the cytosol conductivity σ_2 on the behavior of the function T. The results are given in Figure 5 (cf. with Figures 2 and 3 from ref 33). In particular, we see that there are two relaxation terms when $\sigma_0 = \sigma_2$ (then $\varepsilon_0 = \varepsilon_2$ and hence the system is two-phase). At the same time, one more (high-frequency) term is clearly seen when $\sigma_2 > \sigma_0$. These results evidence that a change in the cytosol conductivity can result in a qualitative transformation of the dielectric spectra.

V. Comments on Application of the Representation

It is pertinent and instructive to briefly discuss our results in the context of possible biological and medical applications. As was noted earlier, the value of the spectral representation is that the material parameters and the geometrical parameters of the medium under consideration are separated. It allows one to analyze them independently. Let us illustrate this with reference to biological cells.

If to consider the material parameters, of most interest are the complex membrane permittivity ε_1 (or permittivities, in the case of multishelled models) and complex cytoplasm permittivity ε_2, which in turn affect the equivalent dielectric constant ε_e. Actually, both direct dependencies $\varepsilon_{\mathrm{eff}}(\varepsilon_1, \varepsilon_2)$ and inverse dependencies $\varepsilon_{1,2}(\varepsilon_{\mathrm{eff}})$ could be of interest.

There are numerous examples showing how diverse factors can affect the dielectric properties of biocell suspensions, especially the permittivity and conductivity of the membranes. The first example is such a phenomenon as electroporation,[34] consisting in a significant increase in the electrical conductivity of the cell membrane caused by an external electric field. At present, electroporation is widely used, in particular, for the electro-uptake of ionic compounds by single cells, gene transfection, and drug delivery. At the same time, the theory of electroporation is not well developed, that hampers the interpretation of respective experimental data.

The second example is the adsorption of metal ions by bacteria and archaea that can be accompanied by a simultaneous change of the permittivity and conductivity of the cell components.[35] Similar to this, the conductivity of the extracellular medium may change due to leakage of ions through the cytoplasmatic membrane or due to ion uptake in the cytoplasm.[36,37] The third example is an interaction between the red blood cells (RBCs) and vascular prostheses made of artificial polymers that can result in a marked alteration (an increase) of both the cell membrane conductivity and permittivity.[38] Assumingly, the effect is due to the membrane-grafted material surface interactions that can modify the structure and composition of the lipid bilayer of the cell membrane. An alteration of the electrical parameters of the cell membranes can be made possible by heating[39,40] or exposure of biocells to the strong magnetic field[41] and gamma-irradiation.[42] Finally, a number of studies show that the dielectric permittivity, capacitance, and conductivity of the white blood cell membranes are higher for the normal cells than those for the malignant ones.[43,44]

Recently, a method has been proposed for the study of membrane lipid bilayers based on dielectric measurements of liposome solutions.[45] It is obvious that our approach is consistent with the above method providing, in addition, a more adequate effective medium theory.

Speaking about the geometry of the cell suspensions, we would like to distinguish two different effects. The first one consists in an alteration of the cell shape resulting from the action of various stimuli. For example, the regular shape of RBCs (biconcave disk) can change into a crenated shape, a sphere, a cup, and other shapes resulting from pH, osmotic pressure, ionic strength, and presence of various reagents.[46] In this connection, mention may be made of blood disorders, such as hereditary and nonhereditary spherocytosis, ovalosytosis, and sickle cell anemia.[47] So, spherocytosis is characterized by the production of the bizarre RBCs that are sphere-like shaped rather than biconcave-disk shaped normal RBCs. Ovalocytosis is characterized by the production of the red blood cells having an abnormal slightly oval or ellipsoidal shape. In the case of sickle-cell anemia, the RBCs are characterized by a rigid, sickle shape. Furthermore, the healthy biconcave-disk shaped red blood cells can be transformed into spinous echinocytes due to high pH[48] or preservation of the blood.[49] Finally, the RBC shape can be changed due to an action of drugs.[50]

The second effect is the cell aggregation. In this case, strong intercellular interaction is capable to significantly change the effective dielectric response of cell suspensions. So, the effect was illustrated by the example of RBCs,[51,52] and the similar effect was considered for budding yeast cells using the model of two connected spheres.[33] It should be also noted that aggregation of biocells can, generally speaking, result in their shape change.[53]

Thus, the properly designed dielectric spectroscopy is of interest from the point of view of biological applications, providing us with information on biological functions of the cells, as well as from the point of view of medical applications, including both diagnosis and treatment.[54] Dielectric measurements (especially, when combined with other techniques) are considered to be potentially useful for detecting human disease states, in particular for the early detection of malignancy.

To conclude this section, it should be noted that our approach could be also useful for the study of viruses. Indeed, many viruses are known to have a layered structure including a core (DNAs/RNAs), an envelope, and a capsid layer between them.[55] In principle, although it is not always easy and convenient, their electrical properties can be considered using dielectric spectroscopy. At the same time, because the viruses are usually ranging in size from 20 to 250 nm, their optical properties may be considered in the long wavelength approximation in the visible and infrared range, that is, in terms of the effective medium, using the spectral density function approach. The same can also take place for sufficiently small cells in the infrared range as the approximation is valid.

VI. Concluding Remarks

The main result of this paper tells us how to extend the two-phase spectral representation to three-phase and more complicated multiphase systems such as suspensions of biocells, that is, core−shell particles with a very thin shell or, to be more exact, with a very low volume fraction of the shell. The question then arises, apropos of the present result, what should we do if the shell is not very thin.

Before answering this question it should be reminded that we have considered the shell thickness to be very small for the sake of convenience of mathematical treatment. As already noted, such an assumption seems to be reasonable in many practical cases due to very small thickness of real cell membranes. However, it is not the case when dealing with some multishell models, as at least one of the shells is not very thin. For example, bacteria, yeast, and plant cells usually have the so-called cell wall (an additional shell) outside the membrane.[56] Correspondingly, the dielectric properties of such biocells may be considered in terms of the two-shell model. Thus, in this case we should use eq 6, where L_2 is a function of L_1. The relation between the depolarization factors of outer (L_1) and inner (L_2) confocal spheroids is signified implicitly.[57] In the general case, dealing with the multishell model, we should use eq 6 iteratively taking into account that L_i is a function of L_{i-1}.

Because the conventional impedance dielectric spectroscopy deals with the measurements on cell suspensions, it gives us assembly averaged (effective) dielectric properties of the cell collections. At the same time, we usually need some useful information on single cells. So, in the recent years more emphasis has been placed on the development of various techniques feasible for single cell analysis;[58] it is the current trend in biological and medical researches. Such techniques, while promising, are yet much more complicated and time-consuming than the conventional dielectric spectroscopy. Thus, extracting single cell information from the dielectric spectra of cell suspensions continues to be relevant. If the mixing rule is known, the problem becomes trivial because it reduces to a standard fitting procedure for the dielectric parameters of the cells. In the general case, however, it is not so, because the spectral density function is usually unknown. It means that before extracting the cell dielectric parameters we should first determine the function for the cell suspension under consideration. Some approaches to this problem have been proposed.[59] In general, the spectral density can be determined using relevant experimental data.[60] As was noted earlier,[61] this procedure belongs to the class of the so-called ill-posed problems and a correct solution is possible only with the use of stabilization techniques. Mention may be also made of the work based on an expansion of the modified spectral density function in terms of Legendre polynomials,[62] the reconstruction of the spectral density function using Padé approximation derived from a constrained minimization problem,[63] as well as of Tuncer's approach[6,64] based on the Monte Carlo integration and constrained least-squares algorithm. In principle, it seems possible not only to extract the spectral density function from experimental data, but also to obtain the volume fractions and effective shapes of inclusions.[64]

In summary, an extension of the spectral density function approach is proposed and discussed that can be applied to interpretation of the dielectric spectra of shelled particles such as biological cells. For illustration, some simple examples of the density function, as well as possible applications, are considered.

Acknowledgment. The authors are indebted to Cesare Cametti, who kindly provided us with the dielectric spectra of suspensions of red blood cells.

References and Notes

(1) Considering the counts of the term "dielectric spectroscopy" with the use of ISI's databases, we have found that the number of the respective scientific publications grows roughly linearly with time, with a faster acceleration during the last two years.
(2) Asami, K. *Prog. Polym. Sci.* **2002**, *27*, 1617–1659.
(3) See e.g. Young, K. D. *Microbiol. Mol. Biol. Rev.* **2006**, *70*, 660–703.
(4) Vrinceanu, D.; Gheorghiu, E. *Bioelectrochem. Bioenerg.* **1996**, *40*, 167–170, It should be noted that the authors, in essence, have rederived the result of Fuchs (see ref 12).
(5) Di Biasio, A.; Ambrosone, L.; Cametti, C. *J.Phys. D: Appl. Phys.* **2009**, *42*, 025401. The method makes use of an algorithm proposed earlier by Prodan and Prodan (see Ref 15).
(6) Tuncer, E.; Serdyuk, Y. V.; Gubanski, S. M. *IEEE Trans. Diel. El. Insul.* **2002**, *9*, 809–828.
(7) Bergman, D. J. *Phys. Rep. C* **1978**, *43*, 377–407.
(8) Milton, G. W. *Appl. Phys. Lett.* **1980**, *37*, 300–302.
(9) See e.g., Lei, J.; Wan, J. T. K.; Yu, K. W.; Sun, H. *Phys. Rev. E* **2001**, *64*, 012903The relationship between the spectral representation and dielectric relaxation is shown in Tuncer E. *J. Phys.: Condens. Matter.* **2005**, *17*, L125-L128.
(10) Huang, J. P.; Yu, K. W.; Lei, J.; Sun, H. *Commun. Theor. Phys.* **2002**, *38*, 113–120.
(11) Dong, L.; Karttunen, M.; Yu, K. W. *Phys. Rev. E* **2005**, *72*, 016613.
(12) Fuchs, R. *Phys. Rev. B* **1975**, *11*, 1732–1740.
(13) Golden, K.; Papanicolaou, G. *Commun. Math. Phys.* **1983**, *90*, 473–491.
(14) Goncharenko, A. V.; Lozovski, V. Z.; Venger, E. F. *J. Phys.: Condens. Matter* **2001**, *13*, 8217–8234.
(15) Prodan, C.; Prodan, E. *J. Phys. D: Appl. Phys.* **1999**, *32*, 335–343.
(16) Tuncer, E.; Bowler, N.; Youngs, I. J. *Physica B* **2006**, *373*, 306–312.
(17) Bohren, C. F.; Huffman, D. R. *Absorption and Scattering of Light by Small Particles*; Wiley: New York, 1983.
(18) Skryabin, I. L.; Radchik, A. V.; Moses, P.; Smith, G. B. *Appl. Phys. Lett.* **1997**, *70*, 2221–2223.
(19) Goncharenko, A. V. *Appl. Phys. Lett.* **2007**, *91*, 246101.
(20) Miragliotta, J.; Furtak, T. E. *Phys. Rev. B* **1987**, *35*, 7382–7391.
(21) See e.g., Gao, L. *Phys. Lett. A* **2003**, *318*, 119–125.
(22) Gao, L.; Wan, J. T. K.; Yu, K. W.; Li, Z. Y. *J. Phys.: Condens. Matt.* **2000**, *12*, 6825–6836.
(23) Stroud, D.; Milton, G. W.; De, B. R. *Phys. Rev. B* **1986**, *34*, 5145–5153.
(24) Goncharenko, A. V. *Chem. Phys. Lett.* **2004**, *386*, 462–468.
(25) Bordi, F.; Cametti, C.; Gili, T. *J. Non-Cryst. Sol.* **2002**, *305*, 278–284.
(26) Bonicontro, A.; Cametti, C. *Coll. Surf. A: Physicochem. Eng. Asp.* **2004**, *246*, 115–120.
(27) Goncharenko, A. V.; Lozovski, V. Z.; Venger, E. F. *Opt. Commun.* **2000**, *174*, 19–32.
(28) Ma, H.; Sheng, P.; Wong, G. K. L. *Topics Appl. Phys.* **2002**, *82*, 41–62.
(29) Yang, J.; Huang, Y.; Wang, X.; Wang, X. B.; Becker, F. F.; Gascoyne, P. R. C. *Biophys. J.* **1999**, *76*, 3307–3314.
(30) Huang, Y.; Wang, X. B.; Gascoyne, P. R. C.; Becker, F. F. *Biochim. Biophys. Acta* **1999**, *1417*, 51–62.
(31) Lisin, R.; Ginzburg, B. Z.; Schlesinger, M.; Feldman, Y. *Biochim. Biophys. Acta* **1996**, *1280*, 34–40.

(32) Asami, K.; Gheorghiu, E.; Yonezawa, T. *Biochim. Biophys. Acta* **1998**, *1381*, 234–240.
(33) Sekine, K.; Watanabe, Y.; Hara, S.; Asami, K. *Biochim. Biophys. Acta* **2005**, *1721*, 130–138.
(34) Tsong, T. Y. *Biophys. J.* **1991**, *60*, 297–306.
(35) Bai, W.; Zhao, K.; Asami, K. *Coll. Surf. B: Biointerfaces* **2007**, *58*, 105–115.
(36) Wal, A.; van der Minor, M.; Norde, W.; Zehnder, A. J. B.; Lyklema, J. *J. Colloid Interface Sci.* **1997**, *186*, 71–79.
(37) Yang, L. *Talanta* **2008**, *74*, 1621–1629.
(38) Basoli, A.; Bordi, F.; Gili, T. *J. Biomed. Mater. Res.* **2002**, *59*, 100–109.
(39) Bonincontro, A.; Mariutti, G. *Phys. Med. Biol.* **1988**, *33*, 557–568.
(40) Ivanov, I. T. *Biol. Membr.* **1993**, *10*, 160–169.
(41) Santini, M. T.; Cametti, C.; Paradisi, S.; Straface, E.; Donelli, G.; Indovina, P. L.; Malorni, W. *Bioelectrochem. Bioelectroenerg.* **1995**, *36*, 39–45.
(42) Bonicontro, A.; Cametti, C.; Rosi, A.; Sportelli, L. *Intern. J. Radiat. Biol.* **1987**, *52*, 447–457.
(43) Polevaya, Y.; Ermolina, I.; Schlesinger, M.; Ginzburg, B. Z.; Feldman, Y. *Biochim. Biophys. Acta* **1999**, *1419*, 257–271.
(44) Ermolina, I.; Polevaya, Y.; Feldman, Y.; Ginzburg, B. Z.; Schlesinger, M. *IEEE Trans. Diel. Electr. Insul.* **2001**, *8*, 253–261.
(45) Merla, C.; Liberti, M.; Apollonio, F.; d'Inzeo, G. *Bioelectromagnet.* **2009**, *30*, 286–298.
(46) Nakao, M., In *Blood Cell Biochemistry. Erythroid Cells*; Harris J. R., Ed.; Plenum: New York, 1990; Vol. 1, pp 195−226.
(47) Suresh, S. *J. Mater. Res.* **2006**, *21*, 1871–1877.
(48) Gedde, M. M.; Davis, D. K.; Huestis, W. H. *Biophys. J.* **1997**, *72*, 1234–1246.
(49) Hayashi, Y.; Oshige, I.; Katsumoto, Y.; Omori, S.; Yakuda, A.; Asami, K. *Phys. Med. Biol.* **2008**, *53*, 295–304.
(50) Deuticke, B.; Grebe, R.; Haest, C. W. M., In *Blood Cell Biochemistry. Erythroid Cells*; Harris J. R., Ed.; Plenum: New York, 1990; Vol. 1, pp 475−530.
(51) Sebastian, J. L.; San Martin, S. M.; Sancho, M.; Miranda, J. M.; Alvarez, G. *Phys. Rev. E* **2005**, *72*, 031913.
(52) Asami, K.; Sekine, K. *J. Phys. D: Appl. Phys.* **2007**, *40*, 2197–2204.
(53) Santini, M. T.; Cametti, C.; Indovina, P. L.; Morelli, G.; Donelli, G. *J. Biomed. Mater. Res.* **1997**, *35*, 165–174.
(54) Feldman, Y.; Ermolina, I.; Hayashi, Y. *IEEE Trans. Diel. Electr. Insul.* **2003**, *10*, 728–753.
(55) MacCuspie, R. I.; Nuraje, N.; Lee, S. Y.; Runge, A.; Matsui, H. *J. Am. Chem. Soc.* **2008**, *130*, 887–891.
(56) Asami, K. *J. Non-Cryst. Sol.* **2002**, *305*, 268–277.
(57) See e.g. Goncharenko, A. V.; Chang, Y. C. *Chem. Phys. Lett.* **2007**, *439*, 121–126.
(58) Morgan, H.; Sun, T.; Holmes, D.; Gawad, S.; Green, N. G. *J. Phys. D: Appl. Phys.* **2007**, *40*, 61–70.
(59) Goncharenko, A. V. *Phys. Rev. E* **2003**, *68*, 041108.
(60) Day, A. R.; Thorpe, M. F. *J. Phys.: Condens. Matter* **1999**, *11*, 2551–2568.
(61) Cherkaev, E. *Inv. Prob.* **2001**, *17*, 1203–1218.
(62) Pecharroman, C.; Gordillo-Vazquez, F. J. *Phys. Rev. B* **2006**, *74*, 035120.
(63) Zhang, D.; Cherkaev, E. *Inv. Prob.* **2008**, *16*, 425–445.
(64) Tuncer, E. *Phys. Rev. B* **2005**, *71*, 012101.

JP900703A